Jiangsu University of Science and Technology

Bachelor's Degree Project Report

Topic: A study of the added mass effect on vortex-induced vibration (VIV) for flexible risers based on empirical model

Department	**Naval Architecture & Ocean Engineering**
Subject	**Naval Architecture & Ocean Engineering**
Student	**Yaolin Ge**
Student ID	**14401091**
Supervisor	**ZHOU Hong, WANG Kunpeng**

Jun, 2018

By the signatures below, I hereby certify that all work was conducted independently in terms of writing the report, employing the necessary simulation models and carrying out essential computational verifications.

Yadin Ge

Zhenjiang, China

Jun-2018

Abstract

With the oil industry gradually moving to the deep-sea area, it becomes increasingly important to deploy the deep-water systems in the complicated sea state. The design of the slender deep-sea riser must take the structure-fluid interaction into consideration. Vortex-induced vibration (VIV) may result in the fatigue failure of the structure and reduce the fatigue life of the entire deep-sea system. By reviewing previous researches, this report reviews basic principles and properties of VIV. The time-domain model is applied to predict the VIV response under various conditions with considering the effect of added mass. The primary work of this project is listed as follows:

(1) An overview of research progress on VIV is reviewed. The basic principles and concepts of VIV are explained, and the main non-dimensional parameters affecting VIV are elaborated in detail. The generation and decomposition of hydrodynamic forces due to VIV are analyzed. The related phenomena in VIV, such as lock-in, are described.

(2) The principles and parameters of low mass ratio VIV based on time-domain theory are described in detail. A time-domain model is applied to predict the VIV response based on semi-empirical formula.

(3) The parametric analysis is performed for 40 totally different cases in terms of different flow-profile cases, different tension-force cases and different mass-ratio cases.

All hydrodynamic coefficients are originated from the forced oscillation experiment of the rigid cylinder conducted by Gopalkrishnan in 1993[4]. The focus of this report is to investigate the effect of added mass variation. Hence the interaction between Crossflow (CF) and In-Line flow (IL) is ignored, which can greatly reduce the demand for computation resources. Hopefully, a more practical model with higher accuracy would be of great significance to future progress.

Keywords: vortex-induced vibration; added mass; time-domain; marine riser

Table of Contents

Introduction

With the increasing consumption of oil and gas resources on a global scale and the acceleration of the exploitation of inland resources, deep water oil and gas exploration and development has become a new focus. More countries gradually shift their focus to the ocean. For any non-streamlined object, when there is fluid flow, alternating detached vortices will be generated on both sides of the object, which is called "vortex shedding". Whereas the riser uses circular cross-sections, alternating vortexes generate pulsating pressure, which in turn generates flow and lateral periodic forces, thereby stimulating cylinder to vibrate. Cylindrical vibrations of the cycle will affect the turbulent vortex shape of the wake, and the profile of vortex shedding is the main factor determining the vibration of the column. This fluid-structure interaction is called "Vortex-induced vibration (VIV)". Essentially, vortex-induced vibration is a non-linear, self-excited and self-governed vibration with multiple degrees of freedom. This report applies a time-domain method with considering the effect of added mass variation to investigate the behaviour of rigid cylinders and SCRs.

Methodology

The time domain models usually solve VIV in two steps, pre-analysis and time-domain analysis. Pre-analysis mainly calculates the distribution of the added mass coefficients along the deep-sea riser and the dominant frequencies of each riser element, besides, those parameters obtained from pre-analysis will be used to initialize the time -domain analysis.

Pre-analysis

The riser is a multi-degrees-of-freedom system. Therefore, the modal analysis needs the riser to be discretized to analyze each element of the entire riser. Adding more and more elements can make the numerical solution converge to the exact one of the final responses. Based on the knowledge of structural dynamics, for a system of n degrees of freedom has n characteristic equations or called eigenvalue equations. From those eigenvalue equations the natural frequencies of riser system can be calculated. If arrange them by sequence, there will be first-order frequency or fundamental frequency, second-order frequencies and so forth.

$$f_1 < f_2 < \cdots < f_n \tag{1}$$

$$f_r = \frac{f_i D}{U} \tag{2}$$

For each element, to determine the natural frequencies under the potential excitation mode assumes that if the element is in lock-in region, then the lock-in frequency should be as high as possible to ensure that the excitation force coefficient is large enough to excite the riser constantly. Hence, the corresponding n^{th} nondimensional natural frequency should be as close as possible to the energy center. Fig.1 shows that the energy center of vortex-induced vibration in the crossflow direction is around 0.17, therefore, to determine their corresponding nondimensional frequencies $f_{r1}, f_{r2}, \cdots, f_{rn}$ by using Eq.(2). Then select the nondimensional frequency that has the nearest

value to 0.17 as the corresponding reduced frequency with respect to the natural frequency of the potential excitation mode of the corresponding element. The natural frequency of nth potential excitation mode is the initial dominant frequency of the element, i.e. f_{ini}. To iterate the previous steps until all the elements in the entire riser are calculated to obtain the solution of the initial dominant frequency of each corresponding element.

The initial dominant frequency of each element derived from the previous steps is the nth natural frequency corresponding to the potential excitation mode of the element, but it may not be the final dominant frequency of the element. The dominant frequency of the element needs to be determined. In the time domain analysis, the flow force of the riser can be calculated according to the initial amplitude of preset procedures, so as to stimulate the riser to start to vibrate and obtain the excitation amplitude and frequency of the riser. Those mentioned response calculation parameters obtained from time-domain analysis can determine whether the initial dominant frequency is the final dominant frequency according to the lock-in judgement. However, no time domain calculation has been performed so far, therefore, preliminary calculations cannot be proceeded based on time-domain analysis. This report employs the method of modal analysis by calculating the largest power of each order of excitation modes for each element. SHEAR7[2] provides an approach to estimate the modal energy of each order, Eq.(3).

$$\Pi^r = \frac{|Q_r|^2}{2R_r} \tag{3}$$

Where, Q_r is the modal forces, R_r is the modal damping, it can be obtained from Eq.(4) and Eq.(5) separately. and R_h is the corresponding fluid damping of the corresponding mode, R_s is the structural damping.

$$Q_r = \int_{L'} \frac{1}{2} \rho_f C_L(x, V_{R(x)}) D(x) V^2(x) Y_r(x) dx \tag{4}$$

$$R_r = \int_{L-L'} R_h(x) Y_r^2(x) \omega_r dx + \int_0^L R_s(x) Y_r^2(x) \omega_r dx \tag{5}$$

After finding those calculation frequencies by calculating the excitation mode with the maximum power, and by repeating doing so to cover the entire riser to get the complete calculation frequencies of the entire riser. In order to judge whether the initial dominant frequencies are the final dominant frequencies or not, the lock-in condition must be examined.
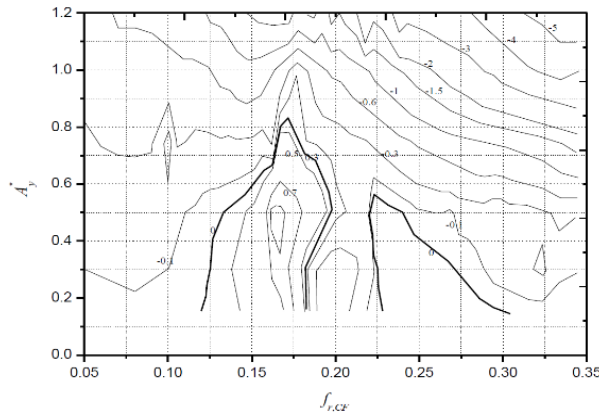

Fig. 1 Excitation force coefficient in the crossflow[4]

(1) If the corresponding nondimensional frequency of the calculation frequencies is in the lock-in interval. i.e. [0.125,0.2]. Hence, the initial dominant frequencies are final dominant frequencies.

(2) If the corresponding nondimensional frequency of the calculation frequencies is out of the range of lock-in interval. Therefore, the calculation frequencies are the final dominant frequencies.

The above calculation will eventually get the final dominant frequency f_n of the entire riser, then the iterative analysis is needed to determine the true dominant frequency and the added mass factor associated with it. By Eq.(2) calculation, all the initial calculation of the dominant frequency f_n corresponding to the equivalent frequency f_r is

$$f_r = \frac{f_n D}{U} \tag{6}$$

By means of the reduced frequency f_r according to Fig.2, the corresponding added mass coefficient C_A can be obtained by Eq.(2-18) to correct the dominant frequency as the true dominant frequency, as Eq.(7).

$$f_{nm} = f_n \sqrt{\frac{m^*}{m^* + C_A}} \tag{7}$$

Then according to the corrected true dominant frequency to obtain the corresponding nondimensional frequency to figure out the new added mass coefficient with related to the true dominant frequency. To make sure that the iteration must converge, this report adopts the average value of two added mass coefficients, and then bring it into iteration. The distribution of added mass coefficients along the riser and the true dominant frequencies of the entire riser has been calculated for the whole riser. Details can be found in flow chart 3.
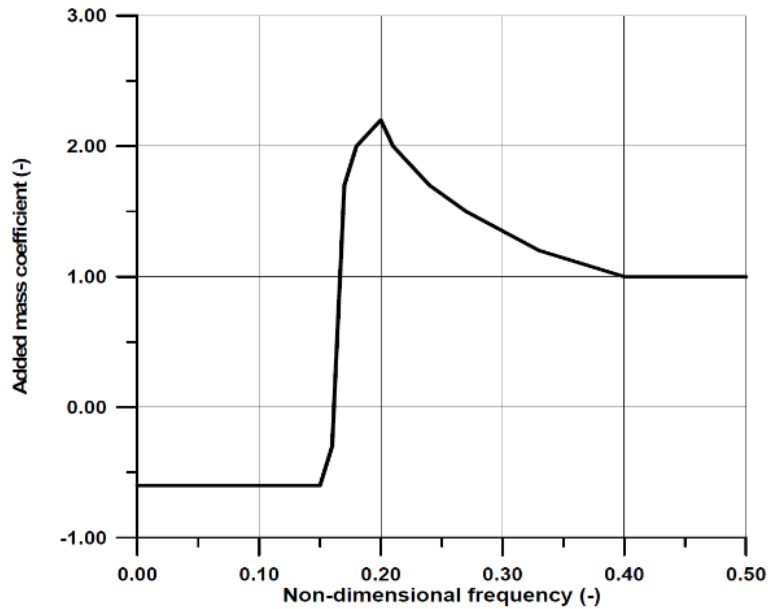

Fig.2 Added mass database as a function of nondimensional frequency
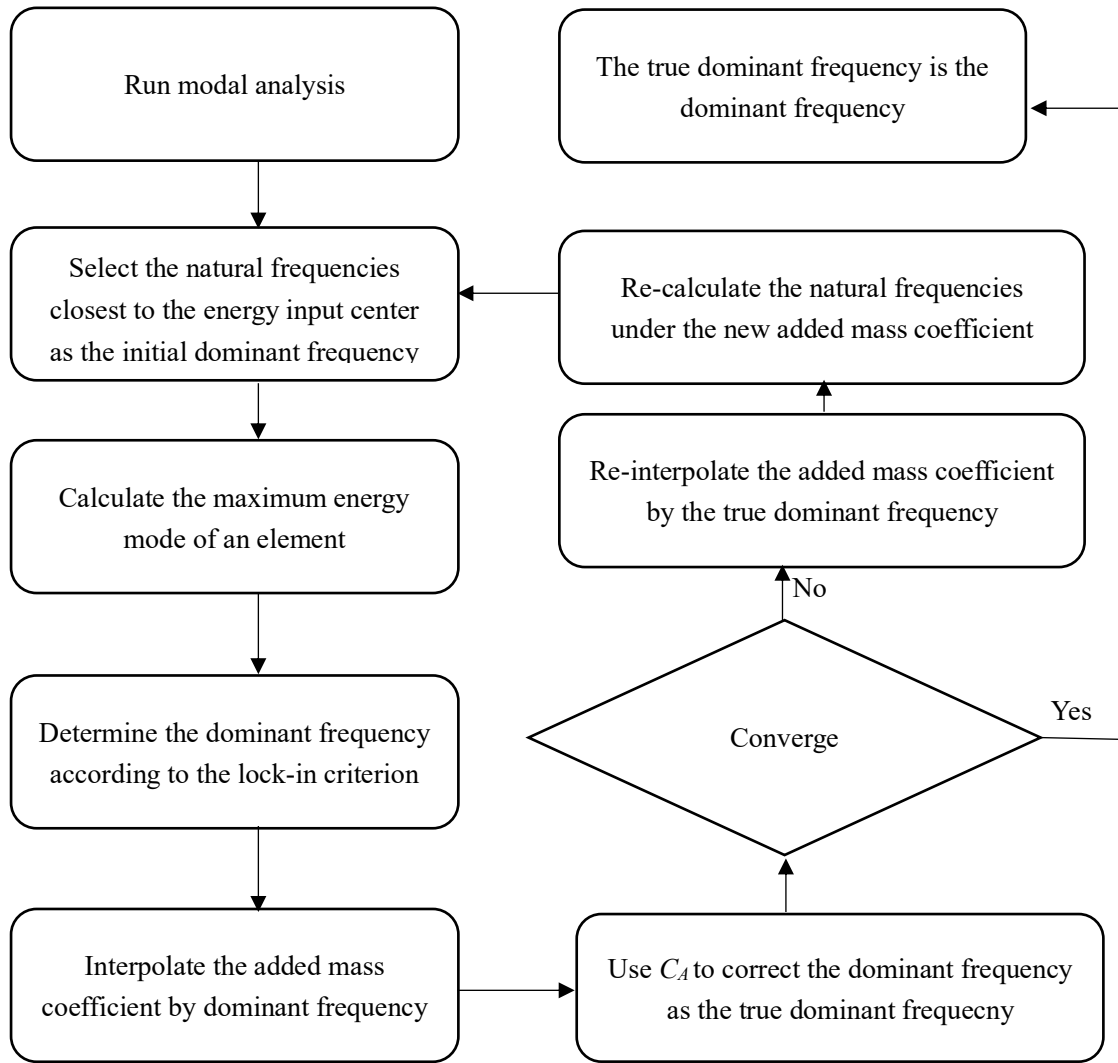
Fig 3. Flow chart of the pre-analysis

Time-domain analysis

It is necessary to use time-domain theory to analyze the vortex-induced vibration of the riser in the case of complex working conditions under the action of ocean currents. At present, the time domain theory analysis method is divided into three categories: Computational fluid dynamics (CFD), Wake oscillator model, and decomposition force model. Among them, the CFD model has the most development prospect, but it still has the shortcoming of the code complexity and the expensive computation resource in the current application [11,12]. The wake oscillator model is described by the Vander Pol Oscillator, the numerical results obtained by the model can be better matched with the experimental results, but it is often very difficult to find out the general parameters used to describe different experiments [4]. The experiment confirms that the added mass coefficient of the vertical riser under uniform flow is not a constant 1.0, and the change of the added mass will not only directly affect the inertia force, but also affect the wet mode [13,14] of the structure. In this report, a decomposition force model is used to analyze the effect of added mass on vortex-induced vibration.

Prerequisite parameters

(1) Excitation coefficient and excitation force

Fig.1 shows the excitation force coefficient obtained from the experimental data of the forced oscillation in the crossflow direction of the rigid cylinder, and with respect to the reduced amplitude $A^* = \dfrac{A}{D}$ and nondimensional frequency $f_r = \dfrac{fD}{V}$. After the excitation force coefficients are obtained, to calculate the crossflow excitation force acting on the riser by using Eq.(8).

$$F_{Hydro} = \frac{1}{2} C_{Lv} \rho_f D V^2 \cos(\omega_n t) \tag{8}$$

(2) Damping coefficient

The damping coefficients involved in this report contain structural damping and hydrodynamic damping, in which structural linear damping is usually expressed as Eq.(9), in which ω is the circular natural frequency of the structure response, and ξ is the critical damping coefficient of the structure.

$$c_s = 2m\omega\xi \tag{9}$$

When the excitation force coefficient C_{Lv} is positive, the excitation force is in phase with the velocity of the structure, so the excitation force drives the riser to vibrate. However, when the excitation force coefficient C_{Lv} is negative, the hydrodynamic damping force dissipates energy from the system, and the hydrodynamic damping coefficient can be expressed as Eq.(10).

$$c_f = -\frac{C_V(A^*, f_r, t)\rho_f V^2}{2A^*\omega} \tag{10}$$

(3) Calculation amplitude and calculation frequency

Through the time-domain analysis calculation, the response displacement of the corresponding node is obtained at each step. According to the above parameters, By using Eq.(11), it can get the calculation amplitude A and calculation frequency f, in which, u_a, u_b, t_a, t_b are calculated according to the response difference of two adjacent time steps, see Fig.4.

$$A = \frac{|u_b - u_a|}{2} \tag{11}$$

$$f = \frac{1}{\left[2 \times (t_b - t_a)\right]} \tag{11}$$
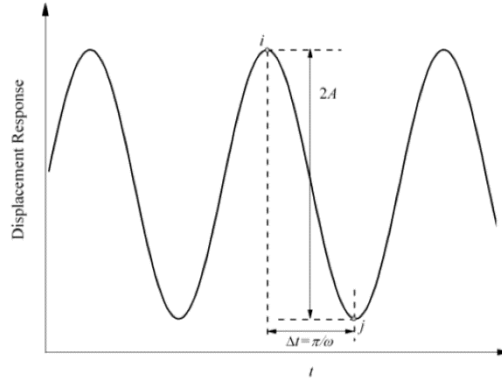

Fig.4 Scheme of response calculation

Prediction model

For a deep-sea riser, it has great slenderness ratio. According to the differential equations of motion, the control equation of vortex-induced vibration of deep sea riser is as follow:

$$(m + \Delta m)\ddot{r} + c\dot{r} + (EIr'')'' - (T_e r')' = F_{Hydro} \tag{12}$$

Where, Δm is the added mass can be obtained from the pre-analysis procedures, and c is the damping coefficient calculated from the above section, F_{Hydro} is the excitation force of vortex-induced vibration. The detailed calculation process is as follows, as shown in the flowchart Fig.5.

(1) According to the dominant frequency f_n obtained from the pre-analysis, the corresponding dimensionless frequency is calculated, and set the initial amplitude value to interpolate the hydrodynamic excitation force coefficients based on Fig.1, and then calculate the hydrodynamic force F_{Hydro};

(2) The added mass coefficient, the parameters of damping and the hydrodynamic force are brought into the control equation Eq.(12) to calculate the calculation frequency and the calculation amplitude of the structure response.

(3) According to its nondimensional frequency of the calculation frequency to determine whether it is locked or not. If it is locked, then the hydrodynamic force would be excitation force, and vice versa, i.e. the hydrodynamic force is the damping force. Hence, to calculate the corresponding force from the corresponding coefficients database.

(4) Set the hydrodynamic force is taken as the initial condition of the next analysis step and the added mass coefficient and damping parameter are used to calculate another structural response until the whole riser is traversed.
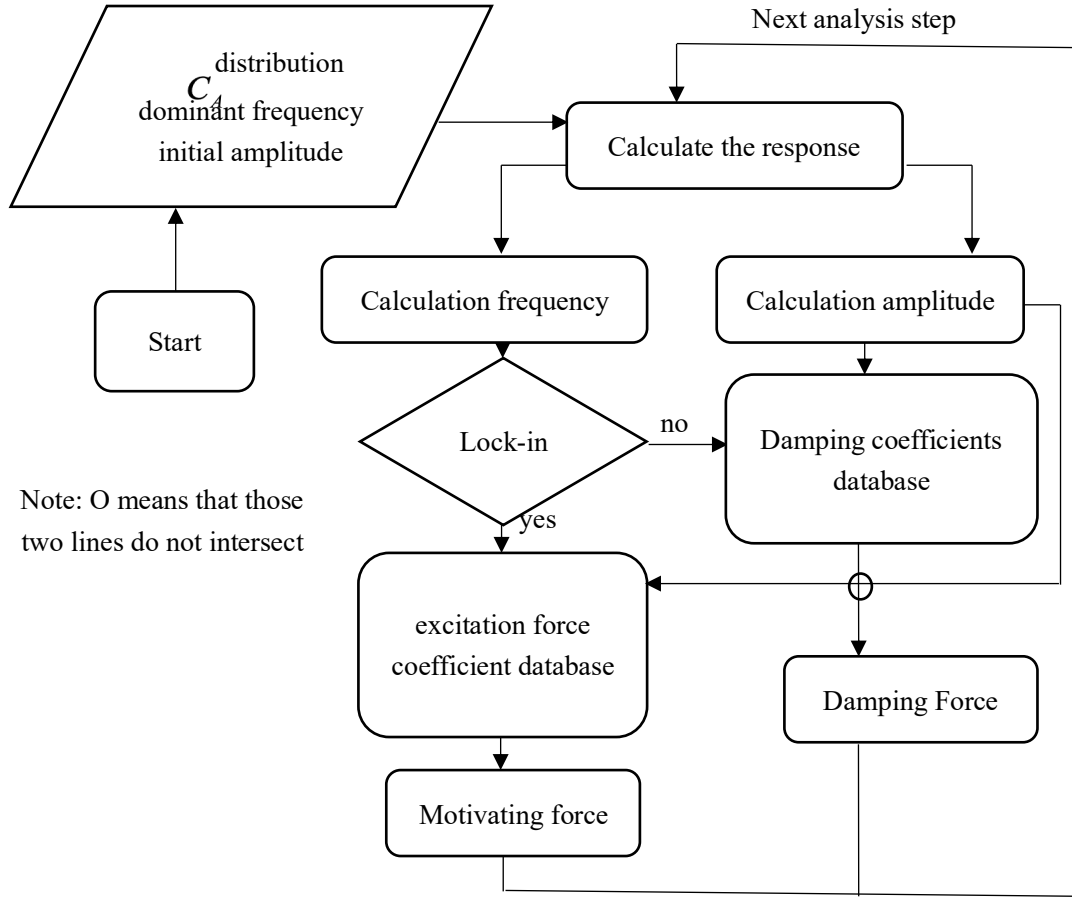
Fig.5 time-domain analysis flowchart

Case study

In order to explore the accuracy and sensitivity of this model, this section conducts sensitivity analysis by selecting 40 different working cases under different flow profiles, different top tension forces and different mass ratios. The SCR riser is selected as the analysed target.

Sensitivity analysis under different flow profiles

Table 1 shows the 15 different working conditions for different flow profiles. The top tension force is 3700N, the mass ratio is 3.13, and the uniform flow velocity are 0.2m/s, 0.3m/s, 0.4m/s, respectively. The estimated envelope curves of the RMS displacement ratio are listed in Figure 6 to 8.

The red line indicates the envelope of the RMS displacement ratio obtained when the added mass coefficient is constant (Ca = 1.0), and the black one represents the displacement obtained by taking into account the added mass variation in the time-domain model. When the flow speed is 0.2m/s, regardless of whether the added mass changes or not, the 5th mode is calculated as the main excitation mode; when the flow speed is 0.3m/s, the same can be obtained whether or not considering the added mass variation can get that the 7th mode is its main excitation mode; when the flow speed increases to 0.4m/s, the 11th mode is estimated without considering the added mass
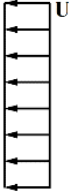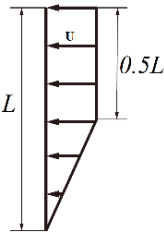
variation while it yields a 10th mode as the main excitation mode as a result of taking the effect of added mass variation.

Figures 9 to 11 show the envelope curves of the RMS displacement ratios of the linear shear flow when the maximum flow speeds are 0.2 m/s, 0.4 m/s, and 0.7 m/s, respectively. When the maximum flow speed is 0.2m/s, the 4th mode is the main excitation mode whether the change of the added mass is considered or not. When the maximum flow speed is 0.4m/s, no matter whether the added mass variation is taken into account or not. The 9th mode is the main excitation mode; when the maximum flow speed is 0.7m/s, the effect of the added mass changes is obvious, but still both are the main excitation modes of the 13th mode.

Figures 12 to 14 show the envelope curves of the RMS displacement ratio at the maximum flow velocity of 0.2 m/s, 0.4 m/s, and 0.7 m/s, respectively, under the step flow conditions. The response of the upper half of the riser is consistent with the characteristics of single mode excitation under uniform flow conditions, while the RMS curve in the lower half of the riser is more inclined to the RMS envelope under shear flow conditions, and meets the characteristics that the multi-modal excitation, besides, added mass changes can bring about greater impact.

Therefore, from the above discussion, for the VIV response of a slender flexible riser in uniform flow, shear flow, or step flow, the order of the excitation mode will increase as the flow velocity increases. At the same time, it can also be obtained that the effect of the added mass to the slender flexible riser in the uniform flow, shear flow, and step flow becomes more pronounced as the flow velocity increases. Worth mentioning, for the vortex-induced vibration response of the riser in a uniform flow, it is a single-mode excitation. The vortex-induced vibration response in the shear flow and step flow is not the same, due to the participation of multiple modes, the resulting envelope curve of the RMS displacement ratio presents an irregular wave.

Table 1 Detailed flow profiles conditions

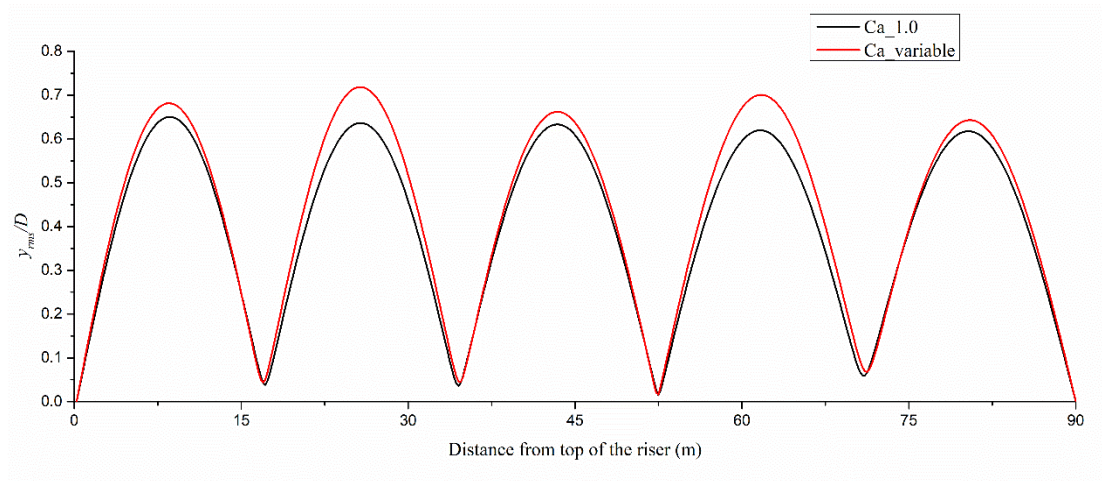| Flow profile	Diagram	Velocity U(m/s)
Uniform flow		0.2
		0.3
		0.4
Shear Flow		0.2
		0.3
		0.4
		0.5
		0.6
		0.7
Step Flow		0.2
		0.3
		0.4
		0.5
		0.6
		0.7

Figure 6 RMS envelope lines of uniform flow condition at 0.2m/s
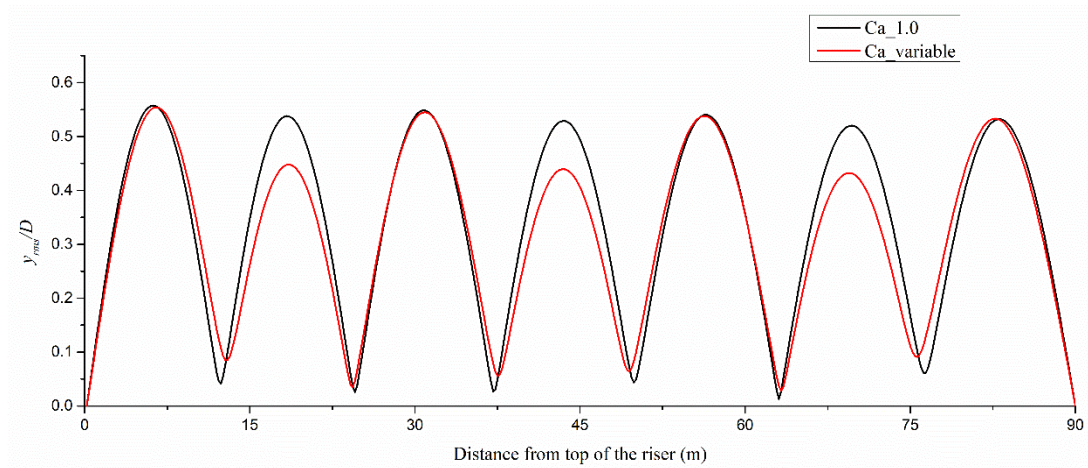

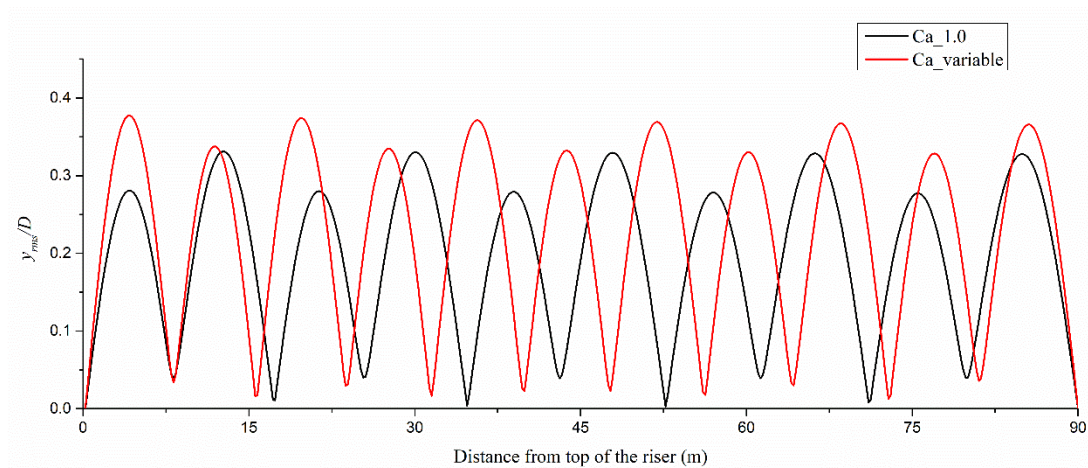Figure 7 RMS envelope lines of uniform flow condition at 0.3m/s

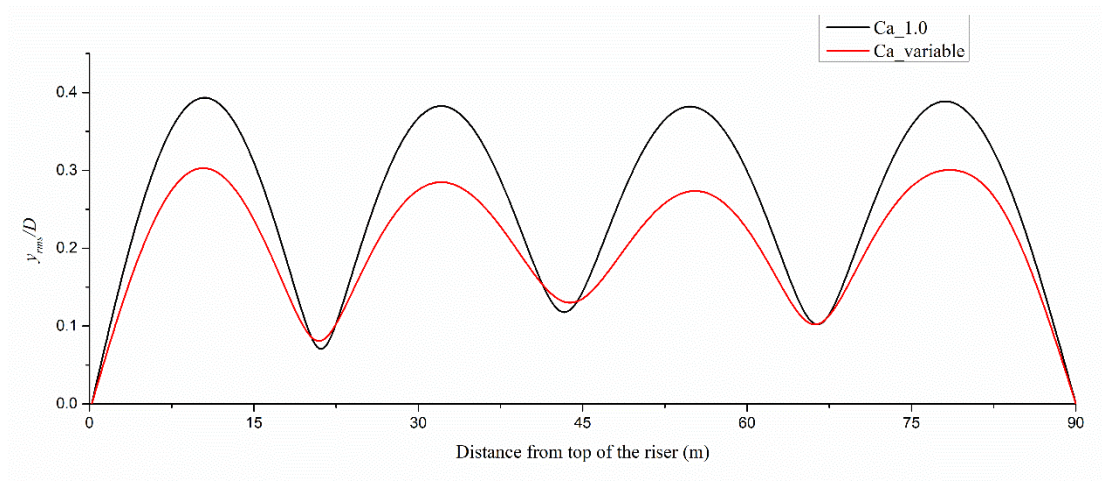Figure 8 RMS envelope lines of uniform flow condition at 0.4m/s

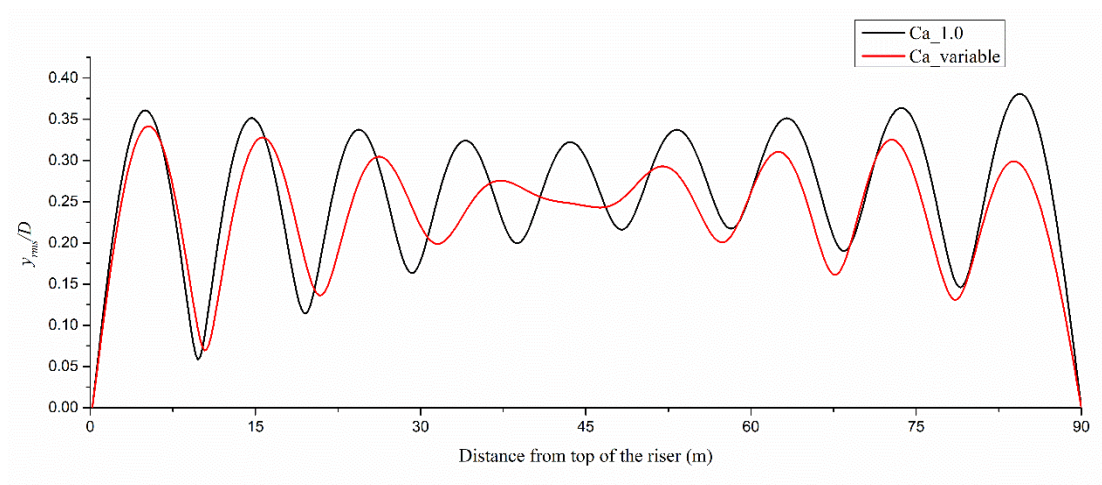Figure 9 RMS envelope lines of shear flow condition at 0.2m/s

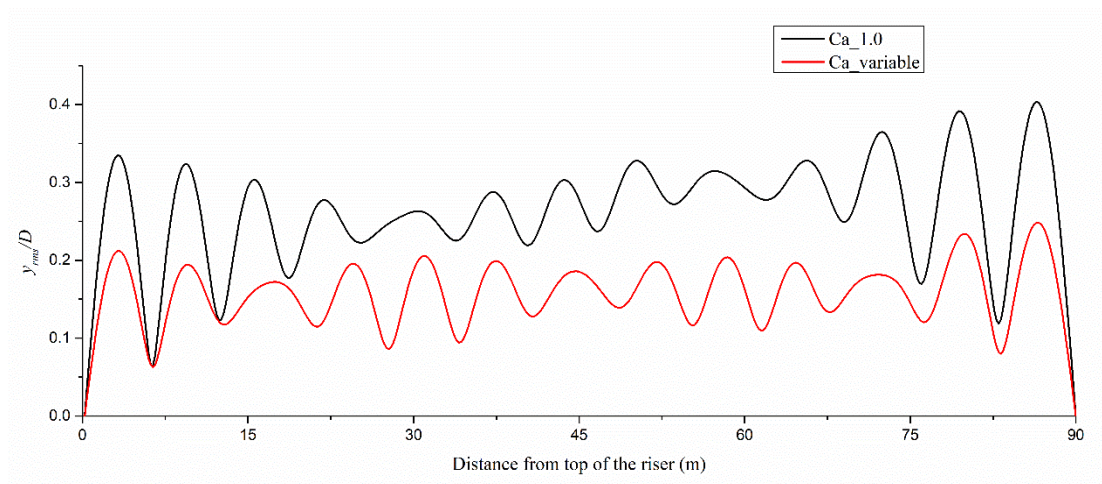Figure 10 RMS envelope lines of shear flow condition at 0.4m/s

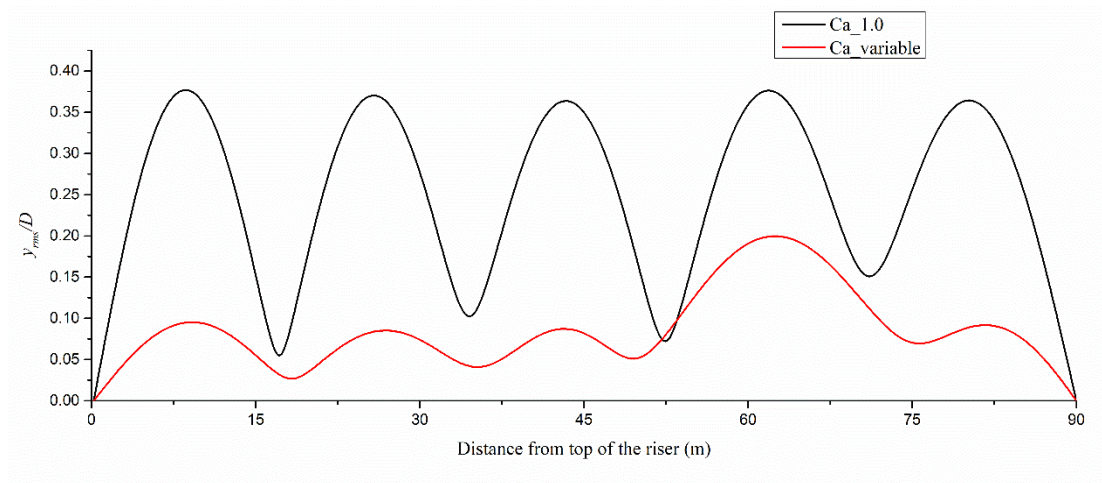Figure 11 RMS envelope lines of shear flow condition at 0.7m/s

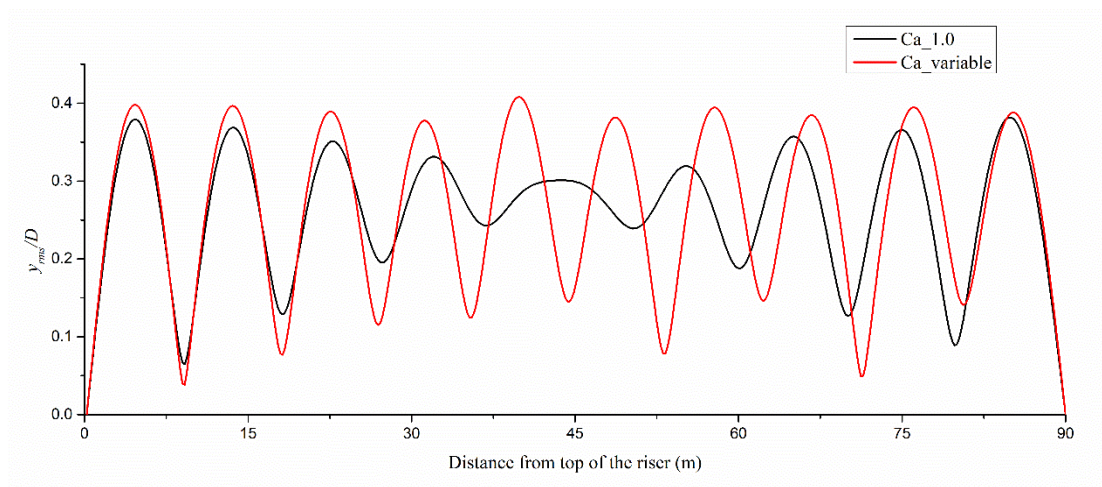Figure 12 RMS envelope lines of step flow condition at 0.2m/s

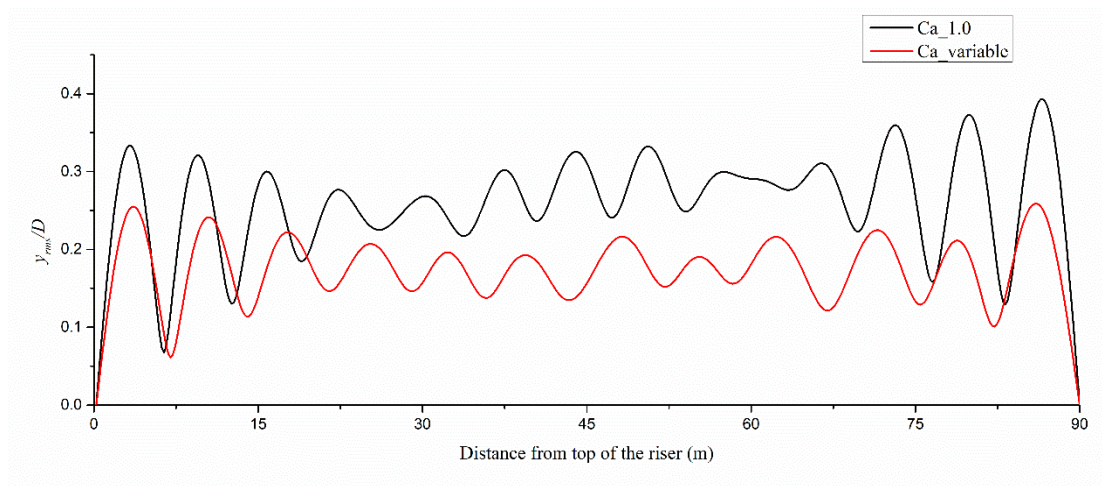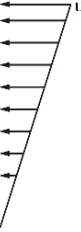Figure 13 RMS envelope lines of step flow condition at 0.4m/s

Figure 14 RMS envelope lines of step flow condition at 0.4m/s

Sensitivity analysis under different tension forces

Table 2 top tension offset table

Flow profile	Speed U(m/s)	Top Tension Force (N)								
	0.4	2700	3000	3300	3600	3900	4200	4500	4800	5100
	0.6	2700	3000	3300	3600	3900	4200	4500	4800	5100

The sensitivity analysis of the of the time-domain model under different top-tension-force cases is discussed in the following section, Table 2 is the offset force data at the linear shear flow of 0.4 m/s and 0.6 m/s, respectively. The response of the riser is predicted from 18 operating conditions with uniform increments between 2700 and 5100N, and the mass ratio is 3.13. Since the top tension force mainly affects the natural frequency of the riser, it can be divided into the following three categories[17]: When the top tension force is so large, the riser model can be simplified as a tight rope; when the the top tension force is too small, then the bending stiffness of the riser itself plays a dominant role, therefore, it should be analyzed as a beam; when the top tension force is not large or not small, then it is necessary to consider all of those influences.

Figures 15 to 20 are envelope diagrams of RMS displacement ratios under 6 different conditions. When the flow speed is 0.4m/s, the top tension force is 2700N, the 10th-order mode is calculated as the main excitation mode without considering the effect of added mass variation, and the 8th-order mode is the main excitation mode with considering the effect of added mass variation. When the top tension force increases to 4200N, the 7th-order mode is obtained as the main excitation mode without considering the effect of added mass variation, but considering the effect of added mass variation, the 9th mode is the main excitation mode. To increase the top tension force of the riser to 5100N, at this time, regardless of whether the added mass variation is considered, the 8th mode is the main excitation mode.

Therefore, it can be seen that when the top tension force is relatively small, the effect of added mass is more pronounced. Meanwhile, it can be obtained that for the riser, as the top tension force increases, the influence of the tension force on the modal natural frequency becomes more obvious. When the flow speed is 0.6m/s, the corresponding dominating modes at the top tension of 2700, 4200, and 5100 are the 13th, 13th, and 12th modes, respectively. These three conditions are also compared with 0.4 m/s to again verify the effect of the increase in flow velocity on the VIV response.
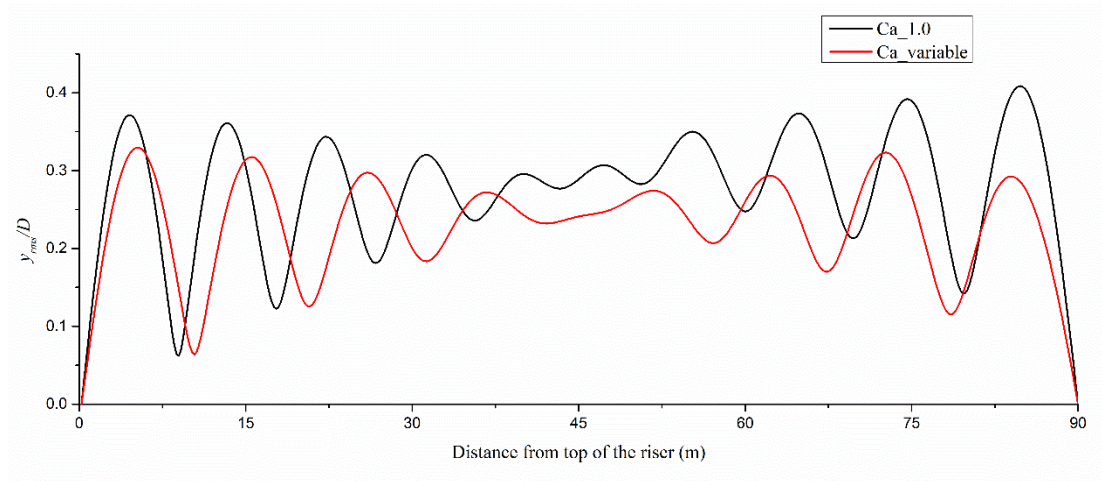
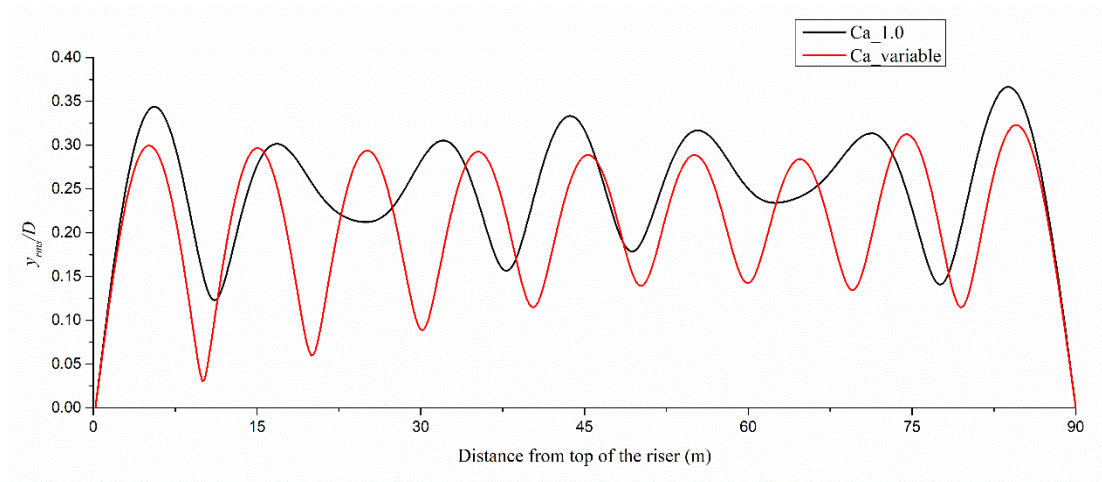Figure 15 RMS envelope lines of shear flow condition at 0.4m/s while TTF 2700N

Figure 16 RMS envelope lines of shear flow condition at 0.4m/s while TTF 4200N

Figure 17 RMS envelope lines of shear flow condition at 0.4m/s while TTF 5100N

Figure 18 RMS envelope lines of shear flow condition at 0.6m/s while TTF 2700N

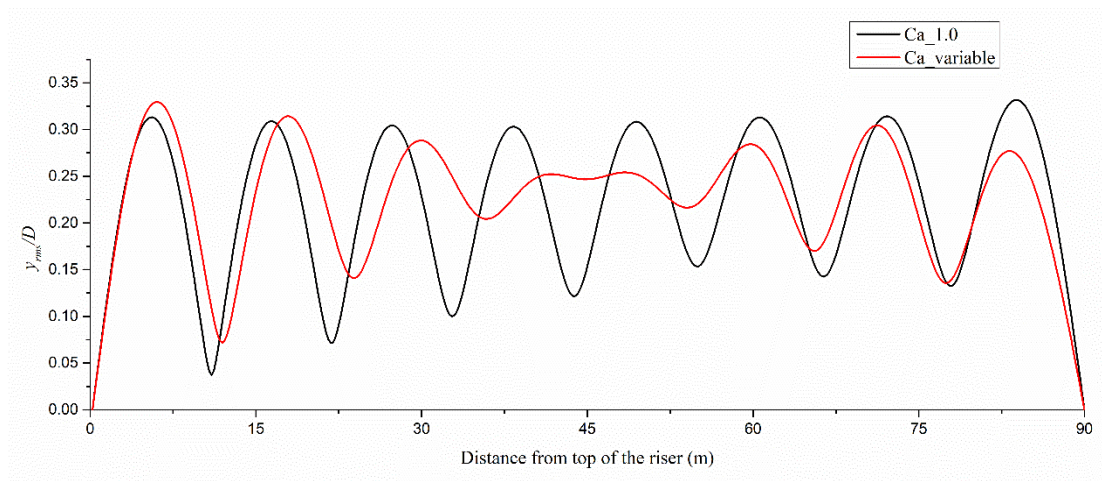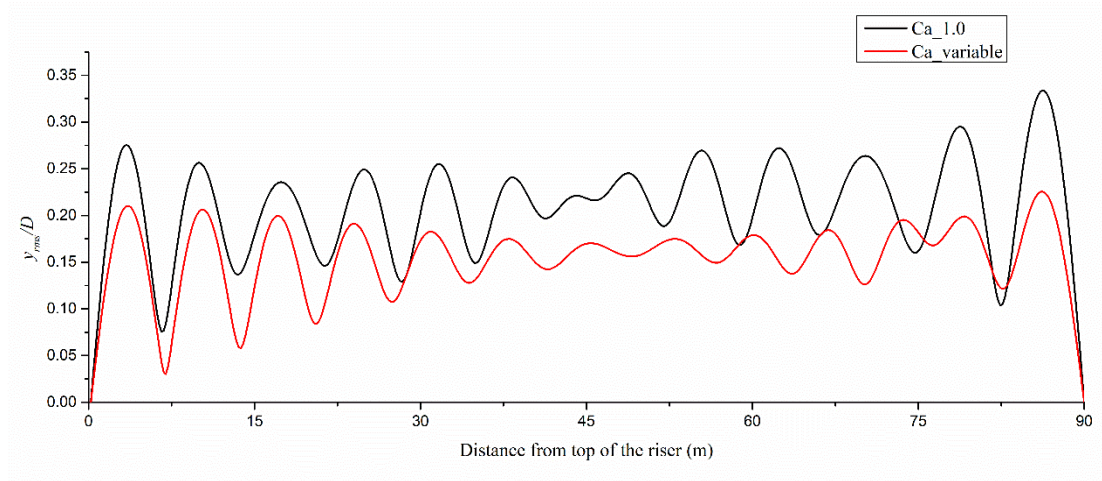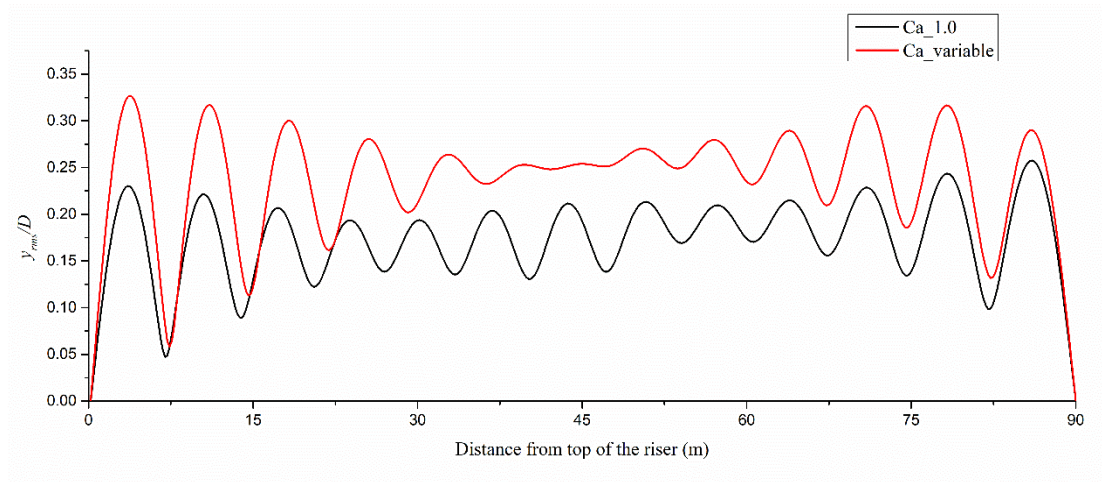Figure 19 RMS envelope lines of shear flow condition at 0.6m/s while TTF 4200N
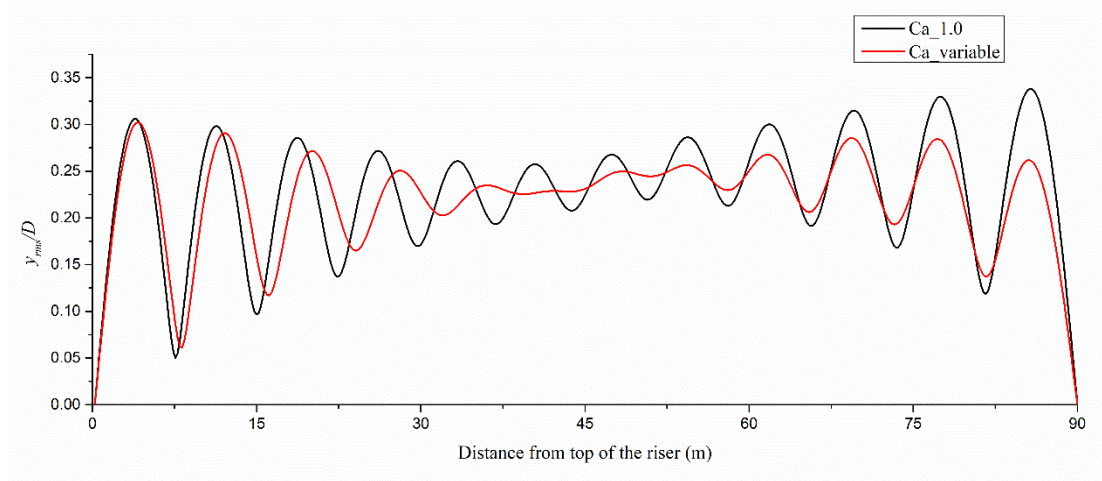

Figure 20 RMS envelope lines of shear flow condition at 0.6m/s while TTF 5100N

Sensitivity analysis under different mass ratios

In order to verify the sensitivity of the time-domain model to the mass ratio under different conditions, seven working conditions with mass ratios from 1.5 to 4.5 are chosen as the targets for

analysing. The top tension force is 3700 N and a linear shear flow with a maximum flow speed of 0.54 m/s is applied.

Figures 21 to 23 show the response RMS displacement ratio envelopes for the three operating conditions with mass ratios of 1.5, 3.0, and 4.5. When the mass ratio is 1.5, the 11th mode is taken as the main excitation mode regardless of the added mass variation, and the mean value of the RMS displacement ratio is approximately 0.3, and the 12th order is obtained when the added mass variation is considered, and the mean value of the RMS displacement ratio is about 0.15, and the effect of added mass makes the average of the RMS displacement ratio reduced to half. When the mass ratio is increased to 3.0, the 13th mode can be obtained as its main excitation mode irrespective of whether the added mass changes or not, but the average value of the RMS displacement ratio is around 0.2 when the added mass variation is not considered, while considering the added mass change, the average value of the RMS displacement ratio is about 0.11, hence, it can be seen that the effect of added mass makes the mean RMS of displacement ratio reduction about half. When the mass ratio continuously increases to 4.5, the 14th mode is taken as its main excitation mode without considering the added mass variation, and the average value of the RMS displacement ratio is about 0.1, and the 15th mode is taken as its main excitation mode with considering the added mass variation, and the mean value of the RMS displacement ratio is about 0.056. The influence of added mass makes the average value of the RMS displacement ratio less than half. From the above comparison, as the mass ratio continues to increase, the effect of added mass on vortex-induced vibration is gradually reduced.
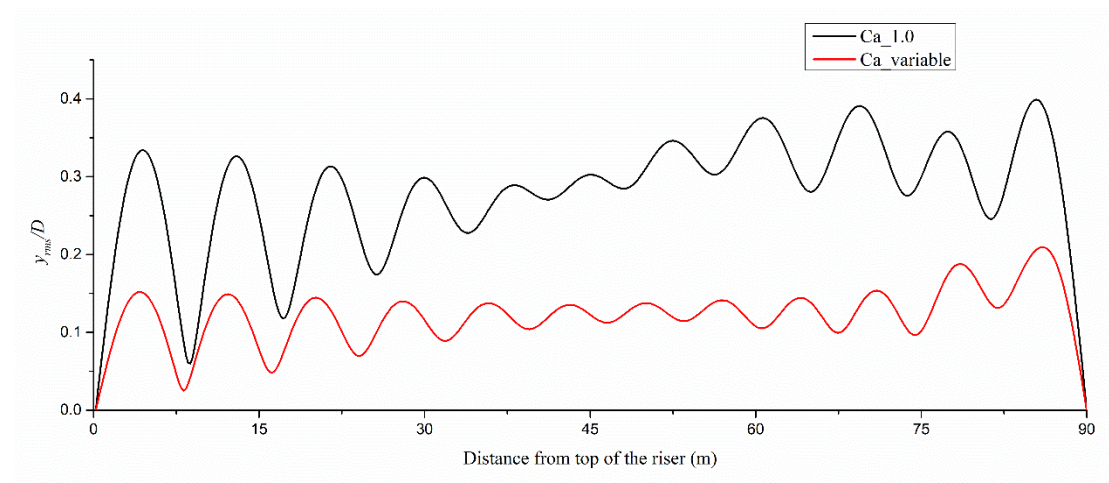

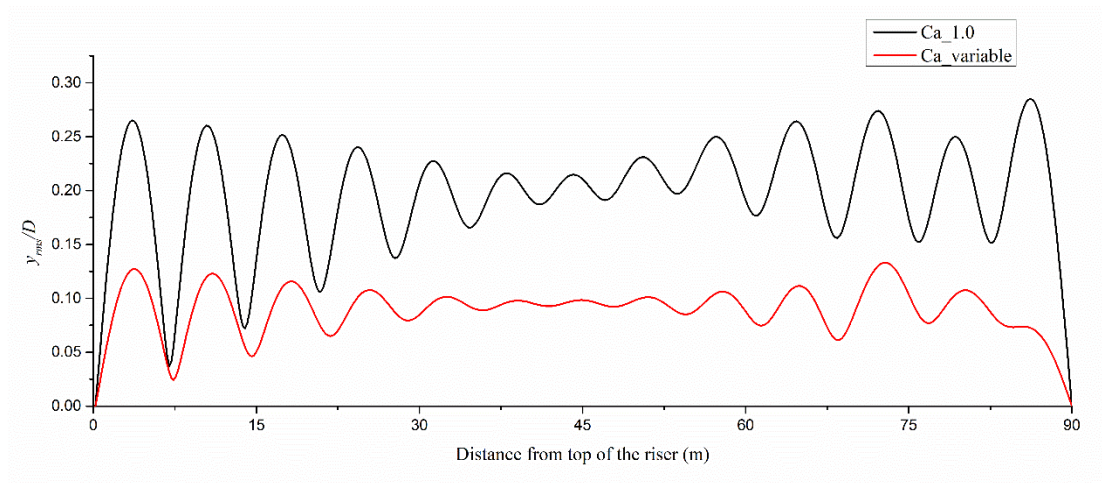Figure 21 RMS envelope lines when the mass ratio is 1.5

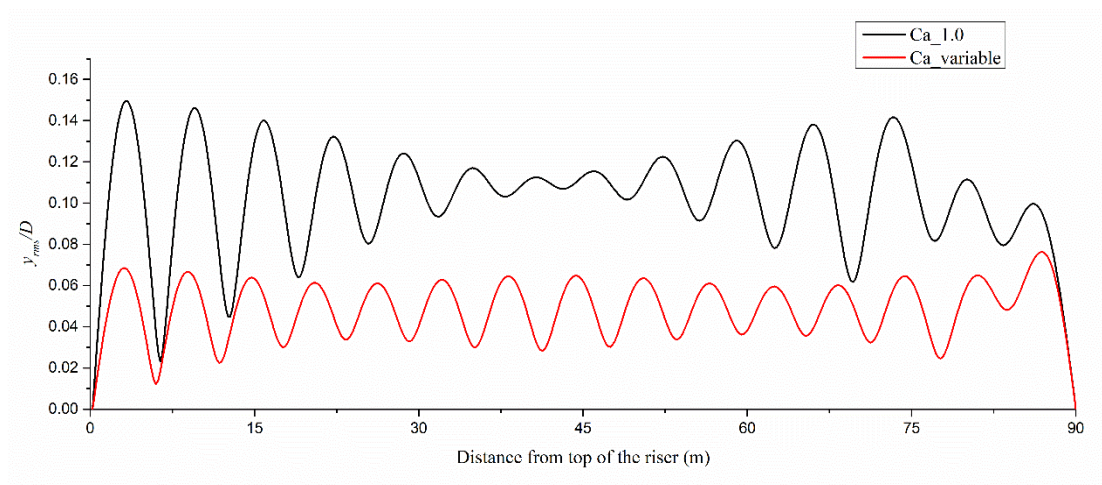Figure 22 RMS envelope lines when the mass ratio is 3.0

Figure 23 RMS envelope lines when the mass ratio is 4.5

Conclusion

The existing vortex-induced vibration prediction methods have not been able to fully grasp the actual response of structures. In this report, according to the experimental data of the forced oscillation experiment of the cylinder, based on the time domain analysis, a prediction model considering the change of added mass is applied. Through the validation analysis of the elastically supported rigid cylinder and the SCR flexible riser, also the sensitivity analysis under different working conditions such as different flow profiles, different top tension forces and different mass ratios, the following conclusions were obtained:

(1) According to the analysis of the basic principles of vortex-induced vibration, it is concluded that the mass ratio and the added mass coefficient are all on the same order of magnitude for the low mass ratio system, and the influence of the added mass is mainly reflected in the natural frequency of the structure. Relative to the high mass ratio system in the air, the influence of added mass is extremely limited. In practice, its influence can often be neglected. It also further explains the importance of considering added mass variation in a low mass ratio VIV system.

(2) The riser system is a multi-degree-of-freedom system, so there are multiple modes from low-order to high-order. When in a uniform flow field, because the flow velocities at the elements are the same and the shedding frequencies are the same, the entire riser is in single-mode excitation and the excitation modes of each element are the same. For shear flow or step flow, since the flow velocity at each element may not be the same, the shedding frequency and its dominant frequency may also be different, so it is in multi-modal excitation.

(4) It can be obtained by analyzing the sensitivity of different flow profile conditions that the excitation mode in any flow field always increases with the increase of flow velocity. According to the sensitivity analysis under different top tension forces conditions, the top tension force mainly affects the determination of the natural frequency of the riser. When the top tension force is large, the riser can be considered as a tight rope and when the top tension force is small, then the riser can be considered as a beam. The sensitivity analysis under different mass ratios conditions shows that as the mass ratio continues to increase, the effect of the added mass variation on the vortex-induced vibration is gradually reduced. The excitation mode of the riser system with a high mass ratio is also high.

Because vortex-induced vibration is influenced by many factors and those factors might interact with each other. The time-domain model can be used to analyze the response of the VIV with considering the added mass variation. Due to the limitations of this report, the current unsolved problems in the industrial field are simplified, for example, the three-dimensional flow problem in complex ocean currents has not been given a suitable model; no sufficient consideration has been given to the mutual movement between elements, only to consider it as a motion within a two-dimensional plane; and the mechanism of turbulence has not yet been fully understood, but it is ubiquitous under actual conditions.

Reference

[1]   Larsen, C.M., Vikestad, K. and Yttervik, R., VIVANA – Theory Manual. MARINTEK, Trondheim, Norway. 2005. pp. 132-144

[2]   Vandiver, J.K., Lee L., User Guide for SHEAR7 Version 4.2. Massachusetts Institute of Technology, Cambridge, Massachusetts, USA. 2002. pp. 132-144

[3]   何长江. 柔性立管涡激振动试验与数值模拟. 哈尔滨工业大学博士学位论文. 2010 年. 5-27

[4]   Gopalkrishnan, R., Vortex induced forces on oscillating bluff cylinders. Doctoral thesis, MIT, Department of Ocean Engineering. 1993. 13-132

[5]   薛鸿祥. 新型深海多柱桁架式平台及立管结构疲劳性能分析. 上海交通大学博士学位论文. 2008 年. 132-144

[6]   潘志远. 海洋立管涡激振动机理与预报方法研究. 上海交通大学博士学位论文. 2005 年. 37-104

[7]   王坤鹏. 深海悬链线立管触底区域及可靠性研究. 上海交通大学博士学位论文. 2014 年. 70-128

[8]   Van Dyke M., An Album of Fluid Motion. The Parabolic Press. 1988: 27-57

[9]   朱仁庆, 杨松林, 杨大明. 实验流体力学. 国防工业出版社. 2005: 13-14

[10]   Lienhard, J.H., Synopsis of lift, drag and vortex frequency data for rigid circular cylinders. Tech. rep., Washington State University, College of Engineering. 1966. pp. 132-144

[11]   Rahman MAA, Leggoe J, Thiagarajan K, Mohd MH, Paik JK. Numerical simulations of vortex-induced vibrations on vertical cylindrical structure with different aspect ratios. Ships Offshore Structures. 2016. 11(4):405–423

[12]   Xu J, Wang DS, Huang H, Duan ML, Gu JJ, An C. A vortex-induced vibration model for the fatigue analysis of a marine drilling riser. Ships Offshore Struct. 2017. 12(S1): S280–S287

[13]   Song LJ, Fu SX, Cao J, Ma LX, Wu J. An investigation into the hydro-dynamics of a flexible riser undergoing vortex-induced vibration. Journal of Fluid Structures. 2016. 63:325–350

[14]   Song LJ, Fu SX, Zeng YD, Chen YF. Hydrodynamic forces and coefficients on flexible risers undergoing vortex-induced vibrations in uni-form flow. J Waterway Port Coast Ocean Eng. 2016. 142(4): 04016001:1–15